2456-8686, x(ii), 2026: 146 - 174
https://doi.org/10.26524/cm243

ORIGINAL RESEARCH **Open Access**

A Discrete-Time Compartmental Model of Problematic Pornography Use Dynamics with Clinical Intervention, Analysed Using Discrete Physics-Informed Neural Networks (D-PINNs)

N. Avinash[1], Nandhini J[2], Janani M[3], Vinothini K[4] and Rikma T[5]

Received: 01 June 2026/ Accepted: 01 July 2026 / Published online: 10 August 2026

Abstract

Continuous-time compartmental models, formulated as systems of ordinary differential equations, are the dominant mathematical framework for describing the population-level dynamics of behavioural-health conditions such as problematic pornography use. In practice, however, the longitudinal data available to clinicians and researchers, periodic clinical-screening waves, survey administrations, or treatment-program intake records, are inherently discrete, sampled at fixed reporting intervals rather than continuously. This paper develops and analyses a discrete-time counterpart to a continuous compartmental model of problematic pornography use dynamics under clinical intervention, formulated directly as a system of nonlinear difference equations rather than as a discretisation applied after the fact. The model partitions a population into four interacting groups, evaluated at discrete reporting indices $n = 0, 1, 2, \dots$: susceptible individuals (S_n), individuals exhibiting problematic or compulsive use patterns (P_n), individuals engaged in clinical treatment (C_n), and recovered individuals (R_n). We establish the positivity and boundedness of solutions, locate the problematic-use-free and persistent-use equilibria, which coincide algebraically with those of the underlying continuous system, and derive the same basic reproduction number $\mathcal{R}_0$ via the Next Generation Matrix method. Local stability is then analysed using the discrete-time Jacobian and the Jury (discrete Routh–Hurwitz) stability criterion, requiring all eigenvalues to lie strictly within the unit circle, a materially different and generally more restrictive condition than the continuous requirement of negative real part. We show analytically that the discrete and continuous

[1]Assistant Professor, Department of Mathematics, Sacred Heart College (Autonomous), Tirupattur, Tamil Nadu, India. Email: avinashprofess@gmail.com
[2]UG Student, Department of Mathematics, Sacred Heart College (Autonomous), Tirupattur, Tamil Nadu, India. Email: nandhinivnb07@gmail.com
[3]UG Student, Department of Mathematics, Sacred Heart College (Autonomous), Tirupattur, Tamil Nadu, India. Email: janani240227@gmail.com
[4]UG Student, Department of Mathematics, Sacred Heart College (Autonomous), Tirupattur, Tamil Nadu, India. Email: vinothinikumar8341@gmail.com
[5]PG Student, Department of Mathematics, Sacred Heart College (Autonomous), Tirupattur, Tamil Nadu, India. Email: rikmarikma399@gmail.com

eigenvalues are related by a unit shift, and derive an explicit, computable sufficient condition under which continuous-time stability at $\mathcal{R}_0 < 1$ carries over to the discrete-time system. To complement this analysis, we implement a discrete Physics-Informed Neural Network (D-PINN) that enforces the governing difference equations directly as a residual loss, without requiring automatic differentiation, and use it to solve the forward and inverse problems from synthetic discretely sampled observational data. The trained network reproduces the forward trajectories with normalized root-mean-square errors below 0.55 across all four compartments, and recovers three of the four unknown parameters with relative error under 10%, while the clinical-intervention-efficacy parameter is markedly more weakly identifiable under discrete, sparser sampling than in the continuous-time formulation, a finding we discuss in detail.

Key words: Problematic pornography use; Discrete-time dynamical systems; Compartmental modeling; Clinical intervention; Jury stability criterion; Discrete Physics-Informed Neural Networks (D-PINNs); Parameter estimation.

AMS classification: 39A30, 92D30, 92B20, 68T07

1 Introduction

Compartmental models of behavioural-health dynamics are almost universally formulated as systems of ordinary differential equations. This is a natural choice mathematically, since it inherits nearly a century of qualitative theory from mathematical epidemiology [6, 7, 8]. It is, however, something of a mismatch with how behavioural-health data are actually collected in practice: clinical screening waves, longitudinal survey panels, and treatment-program intake records are gathered at discrete reporting intervals, weekly, monthly, or at fixed follow-up checkpoints, rather than continuously. A continuous-time ordinary differential equation (ODE) model requires either treating this discretely sampled data as noisy observations of an underlying continuous process, or reformulating the governing dynamics themselves as a discrete-time system whose state transitions occur at exactly the same cadence as the available data.

This paper pursues the second route. We develop a discrete-time counterpart of a continuous compartmental model of problematic pornography use dynamics, formulated directly as a system of nonlinear difference equations indexed by a discrete reporting variable $n = 0, 1, 2, \dots$, representing, for instance, successive weeks of a clinical monitoring program. Rather than treating discretisation as a numerical detail introduced only at the simulation stage, we take the discrete-time map itself as the object of mathematical study: we derive its equilibria, its basic reproduction number,

2456-8686, x(ii), 2026: 146 - 174
https://doi.org/10.26524/cm243

and, crucially, its local stability conditions using discrete-time stability theory, which differs in an essential way from continuous-time stability theory.

Problematic pornography use, characterised in the clinical literature by a persistent pattern of engagement accompanied by impaired control, continued use despite adverse consequences, and clinically significant personal distress or functional impairment, overlaps substantially with, and is often studied under, the diagnostic umbrella of Compulsive Sexual Behaviour Disorder, formally included as an impulse-control disorder in the World Health Organization's eleventh revision of the International Classification of Diseases (ICD-11) [1, 2]. Despite this growing clinical recognition, quantitative, dynamic models capable of describing how problematic use patterns emerge within a population and respond to clinical or preventive intervention over time remain comparatively underdeveloped relative to the extensive cross-sectional, survey-based, and clinical-assessment literature on prevalence, correlates, and screening instruments [3].

1.1 Why Discrete-Time Stability Is a Genuinely Different Problem

For a continuous-time linear system $\dot{x} = Ax$, local asymptotic stability at an equilibrium requires that every eigenvalue of the Jacobian A have strictly negative real part, i.e. that the spectrum lie in the open left half-plane. For a discrete-time linear system $x_{n+1} = Bx_n$, by contrast, local asymptotic stability requires that every eigenvalue of B have modulus strictly less than one, i.e. that the spectrum lie strictly inside the unit circle in the complex plane. These are geometrically different regions of the complex plane, and a system that is stable in continuous time is not automatically stable once naively discretised: a sufficiently large step size, or sufficiently large-magnitude rate parameters, can push discrete eigenvalues outside the unit circle even when the corresponding continuous eigenvalues have negative real part. This paper takes this distinction seriously rather than treating discretisation as stability-preserving by assumption, and derives explicit, checkable conditions, the discrete analogue of the Routh–Hurwitz criteria known as the Jury (or Schur–Cohn) stability criteria [9, 10], under which the discrete-time model inherits the qualitative stability structure of its continuous-time counterpart.

1.2 Scope of the Paper

We first establish non-negativity and boundedness of solutions of the discrete-time system, using discrete induction. We then locate the equilibria of the system; because equilibria are defined by the vanishing of the net change $X_{n+1} - X_n$, the discrete-time and continuous-time models share algebraically identical equilibria and the same basic reproduction number $\mathcal{R}_0$, computed via the Next Generation Matrix method. What differs is the stability analysis: we derive the discrete-time Jacobian, show that its eigenvalues are related to the continuous-time eigenvalues by a simple unit shift, and use this relationship to derive an explicit sufficient condition, checkable directly from the model parameters, under which continuous-time local stability at $\mathcal{R}_0 < 1$ implies discrete-time local stability of the corresponding difference-equation system. We then implement a discrete Physics-Informed Neural Network (D-PINN), which enforces the governing difference equations as a residual loss evaluated at integer collocation indices, requiring no automatic differentiation. Because the discrete residual only requires the network's output at n and $n + 1$, no derivative computation is required at all. We use the trained D-PINN to solve both the forward problem, reconstructing the discrete trajectories from a modest number of observed reporting points, and the inverse problem, recovering the model's key behavioural parameters directly from discretely sampled, noisy data.

This manuscript uses clinical terminology consistent with the World Health Organization's ICD-11 classification of Compulsive Sexual Behaviour Disorder and with the psychological literature on problematic pornography use. The model and its parameters are intended as a mathematical abstraction for population-level dynamical analysis and are not intended to constitute, or substitute for, individual clinical diagnosis or treatment guidance.

2 Literature Review

A substantial body of clinical psychology and psychiatric literature documents the prevalence, correlates, and clinical presentation of problematic pornography use, typically using validated self-report instruments such as the Problematic Pornography Consumption Scale or the Compulsive Sexual Behaviour Disorder Scale [1]. The inclusion of Compulsive Sexual Behaviour Disorder in the ICD-11 as a recognised impulse-control disorder has provided a formal diagnostic framework for this literature and has stimulated further clinical and epidemiological research [2, 3]. However, being predominantly cross-sectional or clinical-sample-based in design, this literature characterises prevalence and correlates at discrete measurement occasions and is not generally built to describe how a population's problematic-use burden evolves continuously.

Discrete-time analogues of continuous compartmental models have a substantial history in mathematical biology, motivated both by the discrete cadence of real surveillance data and by the distinct qualitative behaviour that discrete-time maps can exhibit even when derived from simple continuous models [4]. Allen's foundational work on discrete-time SIS and SIR epidemic models established the now-standard approach of deriving discrete-time basic reproduction numbers via the same next-generation-type argument used in continuous time, while showing that local stability requires a materially different, and generally more restrictive, algebraic condition than its continuous-time counterpart [4]. Related work has extended discrete-time epidemic modelling to more complex compartmental structures and established general Jury-type stability criteria for the resulting polynomial characteristic equations [5].

The basic reproduction number $\mathcal{R}_0$, and the associated Next Generation Matrix technique for computing it in compartmental systems, originates in mathematical epidemiology [6, 7, 8] and has become the standard threshold quantity separating self-limiting from persistent dynamics in a very broad class of models, well beyond infectious disease. The Jury stability criterion (also known as the Schur–Cohn criterion), which provides necessary and sufficient algebraic conditions for all roots of a real polynomial to lie strictly inside the unit circle, is the discrete-time analogue of the Routh–Hurwitz criterion used throughout the continuous-time literature [9, 10].

Physics-Informed Neural Networks were introduced by Raissi, Perdikaris and Karniadakis as a framework for embedding known governing differential equations directly into a neural network's training objective, enabling accurate solution of both forward and inverse problems even from sparse or noisy data [11, 12]. The discrete-time adaptation used in this paper, in which the physics constraint is instead a difference-equation residual evaluated directly from function values at neighbouring integer indices, requires no derivative computation and is consequently simpler to implement, while remaining faithful to the same underlying philosophy of embedding known governing dynamics into the network's training objective.

2456-8686, x(ii), 2026: 146 - 174
https://doi.org/10.26524/cm243

3 Discrete-Time Model Formulation

The model tracks four state variables, evaluated at discrete reporting indices $n = 0, 1, 2, \ldots$ (for instance, successive weeks of a clinical monitoring program):

- S_n: **Susceptible individuals** at reporting index n – individuals who do not currently exhibit problematic use patterns but are exposed to the population's ambient risk-factor environment.
- P_n: **Individuals with problematic use patterns** at reporting index n – individuals exhibiting impaired control, continued engagement despite adverse consequences, and clinically significant distress or functional impairment.
- C_n: **Individuals in clinical treatment** at reporting index n – individuals actively engaged in clinical treatment or counselling.
- R_n: **Recovered individuals** at reporting index n – individuals who have re-established regulated, non-problematic patterns and exert a protective effect on their peers.

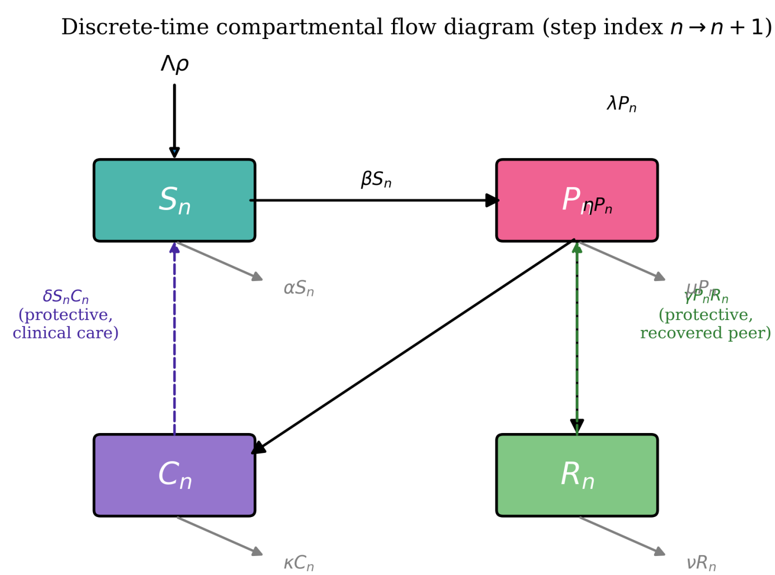

Figure 1: Schematic representation of the discrete-time model architecture, showing the state transition from reporting index n to $n + 1$. Solid arrows denote recruitment, activation, and exit flows; dashed arrows denote the protective (suppressive) feedback exerted by clinical treatment on the susceptible class and by recovered individuals on the problematic-use class.

3.1 Difference Equations

The dynamics of the four compartments are described by the following system of first-order nonlinear difference equations:

$$S_{n+1} = S_n + h\big[\Lambda\rho - \delta S_n C_n - \alpha S_n\big], \tag{1}$$
$$P_{n+1} = P_n + h\big[\beta S_n - \gamma P_n R_n - \mu P_n\big], \tag{2}$$
$$C_{n+1} = C_n + h\big[\eta P_n - \kappa C_n\big], \tag{3}$$
$$R_{n+1} = R_n + h\big[\lambda P_n - \nu R_n\big], \tag{4}$$

where $h > 0$ is the length of one reporting interval in the same physical time units used to calibrate the rate parameters (e.g. $h = 1$ week when all rates are calibrated per week, as in the illustrative simulations of Sections 5–6). Equations (1)–(4) form an explicit forward-difference map: the state at the next reporting index is the current state plus the net rate of change, evaluated at the current state, scaled by the interval length h.

As in continuous-time compartmental models of behavioural spread, the terms βS_n, $\gamma P_n R_n$, ηP_n, and λP_n are phenomenological source-type activation terms rather than literal population transfers: βS_n describes the effective emergence rate of individuals newly exhibiting problematic use, generated by accumulated risk-factor exposure within the susceptible pool, rather than a strict, mass-conserving transfer out of S_n. This modelling principle mirrors the classical within-host viral dynamics model, in which the free-virus population grows through a production term proportional to the infected-cell population without an equal and opposite depletion term in the infected-cell equation [13].

Table: Model parameters, interpretation, and calibration values used in the forward simulations of Sections 5–6. Rates are calibrated per reporting interval (one week), consistent with step size $h = 1$.

Parameter	Description	Value
Λ	Baseline rate of new individuals entering the at-risk cohort, per interval	6250.0
ρ	Proportion of entrants exposed to ambient risk factors	0.80
δ	Preventive/clinical intervention efficacy, protective effect on S_n	2.0×10^{-5}
α	Natural exit rate from the susceptible pool, per interval	0.10
β	Phenomenological activation rate, $S_n \to P_n$, per interval	2.0×10^{-5}
γ	Rate at which recovered-peer influence reduces P_n	1.0×10^{-3}
μ	Natural decline rate of problematic use, per interval	0.08
η	Responsiveness of clinical treatment capacity to P_n, per interval	0.35
κ	Exit rate from the treatment compartment, per interval	0.20
λ	Rate at which recovery grows from P_n, per interval	0.30
ν	Decay rate of the recovered/protected state, per interval	0.12
h	Reporting-interval (step) length	1 (week)

3.2 Relationship to the Continuous-Time Model

Equations (1)–(4) may be recognised as the explicit Euler discretisation, with step size h, of a continuous-time compartmental system. We emphasise, however, that this paper treats the discrete-time map as the primary object of study in its own right, deriving its equilibria, reproduction number, and, most importantly, its own stability theory directly from the map. As shown in Section 4, the discrete-time stability conditions are not simply a re-statement of the continuous-time conditions: they impose an additional, generally more restrictive, requirement that depends explicitly on the reporting interval h and the magnitude of the model's rate parameters.

4 Qualitative Analysis

In this section we establish the fundamental mathematical properties of the discrete-time System (1)–(4): positivity and boundedness of solutions, the equilibrium structure, the basic reproduction number, and, centrally, local stability via the discrete-time Jury (Schur–Cohn) criterion.

4.1 Positivity and Boundedness

Theorem 4.1 (Positivity and Boundedness) Assume all model parameters are non-negative and that the step size h satisfies

$$0 < h \leq \min\left\{\frac{1}{\delta C_n + \alpha},\ \frac{1}{\gamma R_n + \mu},\ \frac{1}{\kappa},\ \frac{1}{\nu}\right\} \quad \text{for all } n \geq 0,$$

a condition automatically satisfied whenever h is small relative to the largest rate parameter in the model (in particular for the calibration $h = 1$ used in Sections 5–6, given the rate magnitudes of Table 3). Then, for non-negative initial conditions $(S_0, P_0, C_0, R_0) \in \mathbb{R}^4_+$, the solution of System (1)–(4) satisfies $(S_n, P_n, C_n, R_n) \in \mathbb{R}^4_+$ for all $n \geq 0$. Moreover, if

$$m = \min\{\alpha - \beta,\ \mu - \eta - \lambda,\ \kappa,\ \nu\} > 0,$$

then the total population $N_n = S_n + P_n + C_n + R_n$ is uniformly bounded for all $n \geq 0$.

Proof:

Positivity. We proceed by induction on n. The base case $n = 0$ holds by assumption. Suppose $(S_n, P_n, C_n, R_n) \in \mathbb{R}^4_+$ for some $n \geq 0$. From Equation (1),

$$S_{n+1} = S_n\big[1 - h(\delta C_n + \alpha)\big] + h\Lambda\rho.$$

Since $h\Lambda\rho \geq 0$ and, by the step-size condition, $1 - h(\delta C_n + \alpha) \geq 0$, and $S_n \geq 0$ by the inductive hypothesis, it follows that $S_{n+1} \geq 0$. Identical arguments applied to Equations (2)–(4), using the corresponding step-size bounds, give

$$P_{n+1} = P_n\big[1-h(\gamma R_n+\mu)\big]+h\beta S_n \;\geq\; 0, \qquad C_{n+1} = C_n(1-h\kappa)+h\eta P_n \;\geq\; 0, \qquad R_{n+1} = R_n(1-h\nu)+h$$

By induction, $(S_n, P_n, C_n, R_n) \in \mathbb{R}^4_+$ for all $n \geq 0$.

Boundedness. Summing Equations (1)–(4),

$$N_{n+1} = N_n + h\Big[\Lambda\rho - (\alpha-\beta)S_n - (\mu-\eta-\lambda)P_n - \kappa C_n - \nu R_n - \delta S_n C_n - \gamma P_n R_n\Big].$$

Since $S_n, P_n, C_n, R_n \geq 0$ by the positivity result just established, the nonlinear terms satisfy $\delta S_n C_n \geq 0$ and $\gamma P_n R_n \geq 0$, so that

$$N_{n+1} \;\leq\; N_n + h\Lambda\rho - hm\,(S_n + P_n + C_n + R_n) = (1-hm)N_n + h\Lambda\rho,$$

where $m = \min\{\alpha-\beta, \mu-\eta-\lambda, \kappa, \nu\} > 0$, and where $0 < 1 - hm < 1$ under the step-size condition. This is a linear first-order recurrence for N_n with fixed point $N^\infty = \Lambda\rho/m$; iterating,

$$N_n \;\leq\; (1-hm)^n N_0 + \frac{\Lambda\rho}{m}\Big[1-(1-hm)^n\Big].$$

Since $|1 - hm| < 1$, taking $n \to \infty$ gives $\limsup_{n\to\infty} N_n \leq \Lambda\rho/m$. Hence every solution eventually enters and remains in the bounded region $\Omega = \{(S,P,C,R) \in \mathbb{R}^4_+ : S+P+C+R \leq \Lambda\rho/m\}$. ■

4.2 Equilibrium Points

An equilibrium of the discrete-time System (1)–(4) is a fixed point (S^*, P^*, C^*, R^*) satisfying $X_{n+1} = X_n = X^*$ for each state variable X. Since $X_{n+1} - X_n = h \cdot f_X(X_n)$ for each compartment, with f_X the corresponding right-hand side, a fixed point of the discrete-time map exists if and only if $f_X(X^*) = 0$ for every compartment (assuming $h \neq 0$). The discrete-time and continuous-time equilibria are therefore algebraically identical.

Problematic-Use-Free Equilibrium.

$$E_0 = \left(\frac{\Lambda\rho}{\alpha},\ 0,\ 0,\ 0 \right).$$

Persistent-Use Equilibrium. Writing $C^* = (\eta/\kappa)P^*$ and $R^* = (\lambda/\nu)P^*$, P^* solves the cubic

$$\frac{\gamma\lambda\delta\eta}{\nu\kappa} P^{*3} + \left(\frac{\gamma\lambda\alpha}{\nu} + \frac{\mu\delta\eta}{\kappa} \right) P^{*2} + \mu\alpha P^* - \beta\Lambda\rho = 0, \tag{$*$}$$

which, by Descartes' Rule of Signs (the coefficient sign pattern is $(+,+,+,-)$, giving exactly one sign change), has a unique positive root whenever $\mathcal{R}_0 > 1$ (defined below), giving the persistent-use equilibrium

$$E^* = \left(\frac{\Lambda\rho}{\frac{\delta\eta}{\kappa}P^* + \alpha},\quad P^*,\quad \frac{\eta}{\kappa}P^*,\quad \frac{\lambda}{\nu}P^* \right).$$

4.3 Basic Reproduction Number

Because the equilibria of the discrete-time and continuous-time systems coincide, and because the Next Generation Matrix construction depends only on the linearisation of the emergence and exit terms at the problematic-use-free equilibrium, not on whether time is discrete or continuous, the basic reproduction number of the discrete-time system is

$$\mathcal{R}_0 = \frac{\beta\Lambda\rho}{\alpha\mu}. \tag{5}$$

As in the continuous-time model, $\mathcal{R}_0 > 1$ is necessary for the persistent-use equilibrium E^* to be feasible. We show next, however, that $\mathcal{R}_0 < 1$ is no longer sufficient on its own for local stability of E_0 in discrete time.

4.4 Local Stability

The Discrete-Time Jacobian. Write the discrete-time map as $X_{n+1} = F(X_n) = X_n + hf(X_n)$, where $f = (f_S, f_P, f_C, f_R)$ denotes the right-hand side of Equations (1)–(4). The Jacobian of F is

$$DF(S, P, C, R) = I_4 + h\, J(S, P, C, R), \tag{6}$$

where

$$J(S,P,C,R) = \begin{pmatrix} -\delta C - \alpha & 0 & -\delta S & 0 \\ \beta & -\gamma R - \mu & 0 & -\gamma P \\ 0 & \eta & -\kappa & 0 \\ 0 & \lambda & 0 & -\nu \end{pmatrix}.$$

Because $DF = I_4 + hJ$, every eigenvalue ξ of DF is related to an eigenvalue z of J by the exact linear relationship

$$\xi = 1 + hz. \tag{7}$$

This is the key structural fact linking the two stability theories: the discrete-time spectrum is simply the continuous-time spectrum, scaled by h and shifted by 1.

Stability of the Problematic-Use-Free Equilibrium. Evaluating DF at E_0, the characteristic polynomial of $J(E_0)$ factors as $(z+\nu)\,q(z)$, where $q(z) = z^3 + a_2 z^2 + a_1 z + a_0$ is the cubic with

$$a_2 = \alpha + \kappa + \mu, \qquad a_1 = \alpha\kappa + \alpha\mu + \kappa\mu, \qquad a_0 = \alpha\kappa\mu + \delta\eta\mu\,\mathcal{R}_0.$$

By Equation (7), the eigenvalues of $DF(E_0)$ are $\xi = 1 - h\nu$ (always real) and the three roots of

$$p(\xi) = \xi^3 + b_2\xi^2 + b_1\xi + b_0 = 0, \tag{8}$$

with

$$b_2 = ha_2 - 3, \tag{9}$$
$$b_1 = h^2 a_1 - 2ha_2 + 3, \tag{10}$$
$$b_0 = h^3 a_0 - h^2 a_1 + ha_2 - 1. \tag{11}$$

(At $h = 1$: $b_2 = a_2 - 3$, $b_1 = a_1 - 2a_2 + 3$, $b_0 = a_0 - a_1 + a_2 - 1$.)

4.4.1 The Jury (Schur–Cohn) Stability Criterion

For a monic real cubic $p(\xi) = \xi^3 + b_2\xi^2 + b_1\xi + b_0$, the Jury criterion states that all three roots lie strictly inside the unit circle if and only if the following four conditions hold simultaneously:

$$\text{(J1)} \quad |b_0| < 1, \tag{12}$$

$$\text{(J2)} \quad p(1) = 1 + b_2 + b_1 + b_0 > 0, \tag{13}$$

$$\text{(J3)} \quad p(-1) = -1 + b_2 - b_1 + b_0 < 0, \tag{14}$$

$$\text{(J4)} \quad |b_1 - b_0 b_2| < 1 - b_0^2. \tag{15}$$

Theorem 4.2 (Structural simplification of (J2) at $h = 1$) At the reporting-interval calibration $h = 1$, condition (J2) reduces exactly to $p(1) = a_0 > 0$, which holds automatically for all admissible (non-negative) parameter values.

Proof:

Substituting $b_2 = a_2 - 3$, $b_1 = a_1 - 2a_2 + 3$, $b_0 = a_0 - a_1 + a_2 - 1$ into $p(1) = 1 + b_2 + b_1 + b_0$ and collecting terms in a_2, a_1, a_0 separately: the coefficient of a_2 is $1 - 2 + 1 = 0$; the coefficient of a_1 is $1 - 1 = 0$; the coefficient of a_0 is 1; and the constant terms are $1 - 3 + 3 - 1 = 0$. Hence $p(1) = a_0$ exactly, which is positive since $\alpha, \kappa, \mu, \delta, \eta, \mathcal{R}_0 \geq 0$. ■

Condition (J2) is therefore never the binding constraint at $h = 1$; the remaining three conditions, (J1), (J3), and (J4), must be checked explicitly and, unlike the continuous-time Routh–Hurwitz condition, do not reduce to a single inequality of the form $\mathcal{R}_0 < 1$. This is the paper's central qualitative finding: discrete-time local stability of the problematic-use-free equilibrium is a strictly stronger requirement than $\mathcal{R}_0 < 1$, and depends explicitly on the magnitudes of α, κ, μ and not only on their appearance in $\mathcal{R}_0$.

Theorem 4.3 (A sufficient condition for discrete stability from continuous stability) Suppose $\mathcal{R}_0 < 1$ and the continuous-time Routh–Hurwitz condition holds, so that all three roots z_1, z_2, z_3 of $q(z) = z^3 + a_2 z^2 + a_1 z + a_0$ are real or complex with strictly negative real part. If, in addition,

$$h \max_i |z_i| < 2 \qquad \text{and} \qquad h\nu < 2,$$

then all four eigenvalues of $DF(E_0)$ satisfy $|\xi_i| < 1$, and the problematic-use-free equilibrium E_0 is locally asymptotically stable for the discrete-time System (1)–(4).

2456-8686, x(ii), 2026: 146 - 174
https://doi.org/10.26524/cm243

Proof:

Write $z_i = p_i + iq_i$ with $p_i < 0$ by the continuous-time stability assumption. Then

$$|\xi_i|^2 = |1 + hz_i|^2 = (1 + hp_i)^2 + (hq_i)^2 = 1 + hp_i\big(2 + hp_i\big) + h^2 q_i^2.$$

A short rearrangement gives $|\xi_i|^2 - 1 = h\big(2p_i + h|z_i|^2\big)$. Since $p_i < 0$, a sufficient condition for $|\xi_i|^2 - 1 < 0$ is $h|z_i|^2 < -2p_i \leq 2|z_i|$, i.e. $h|z_i| < 2$. Taking the maximum over $i = 1, 2, 3$ gives the stated condition $h \max_i |z_i| < 2$, under which $|\xi_i| < 1$ for every $i = 1, 2, 3$. The fourth eigenvalue, associated with the R-compartment, is $\xi_4 = 1 - h\nu$, which satisfies $|\xi_4| < 1$ whenever $0 < h\nu < 2$, a separate, directly checkable condition. Under both conditions jointly, all four eigenvalues of $DF(E_0)$ lie strictly inside the unit circle, establishing local asymptotic stability of E_0 for the discrete-time system. ■

Remark 4.4 Theorem 4.3 shows that continuous-time stability at $\mathcal{R}_0 < 1$ is not automatically inherited by the discrete-time system; an additional condition bounding the product of the step size h and the magnitude of the slowest continuous-time eigenvalue is required. In practice, for behavioural-health applications where rate parameters are calibrated in physically meaningful units (per week, as in Table 3) and are consequently small in magnitude ($|z_i| \ll 1$ for all i in our calibration), the condition $h \max_i |z_i| < 2$ is satisfied with a wide margin at $h = 1$, and discrete-time stability follows from continuous-time stability in practice.

Remark 4.5 (Numerical verification for the calibrated parameter set) For the parameter values of Table 3 at $h = 1$, $a_2 = 0.38$, $a_1 = 0.044$, $a_0 \approx 1.607 \times 10^{-3}$. Solving the cubic Equation $(*)$ numerically at $\mathcal{R}_0 = 12.5$ yields the unique positive root $P^* \approx 9.5864$, giving the persistent-use equilibrium $E^* \approx (49832.80,\ 9.5864,\ 16.776,\ 23.966)$. The continuous eigenvalues of $J(E^*)$ are $z \approx -0.2005, -0.1008, -0.1115 \pm 0.0534i$, giving $\max_i |z_i| \approx 0.2005 \ll 2/h = 2$. The corresponding discrete-time eigenvalues, computed directly as $\xi_i = 1 + z_i$, are

$$\xi_1 \approx 0.7995, \quad \xi_2 \approx 0.8992, \quad \xi_{3,4} \approx 0.8885 \pm 0.0534i,$$

all of which satisfy $|\xi_i| < 1$, confirming that E^* is locally asymptotically stable for the discrete-time system at the calibrated parameter values, consistent with Theorem 4.3.

2456-8686, x(ii), 2026: 146 - 174
https://doi.org/10.26524/cm243

We further verified all four Jury conditions (J1)–(J4) directly and numerically at E_0's cubic coefficients: $|b_0| = 0.662 < 1$; $p(1) = a_0 = 0.00161 > 0$; $p(-1) = -6.566 < 0$; and $|b_1 - b_0 b_2| = 0.549 < 1 - b_0^2 = 0.561$, confirming all four conditions hold. Figure 2 plots the eigenvalues relative to the unit circle.

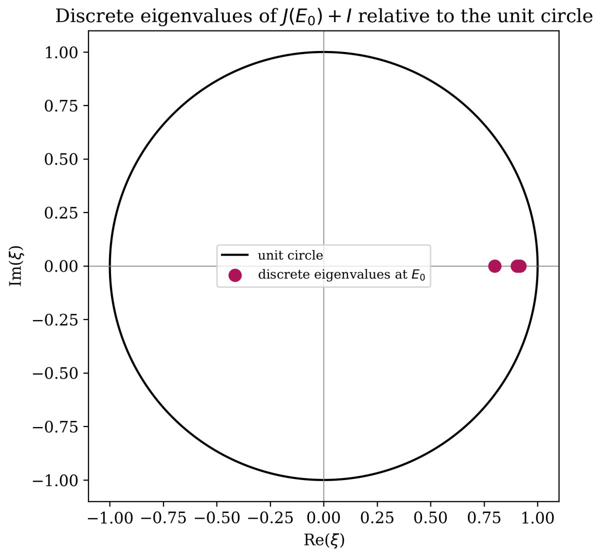

Figure 2: Discrete-time eigenvalues of DF at the calibrated equilibrium, plotted in the complex plane relative to the unit circle. All eigenvalues lie strictly inside the unit disk, confirming local asymptotic stability.

Stability of the Persistent-Use Equilibrium. The same eigenvalue-shift relationship $\xi = 1 + hz$ applies at E^*, where the relevant characteristic polynomial is a full quartic rather than a cubic-times-linear-factor. The discrete-time Jury criterion for a monic quartic requires four analogous conditions [9, 10], which we verify numerically for the calibrated parameter set in Remark 4.5 above; the same eigenvalue-shift argument used in Theorem 4.3 extends directly to the quartic case, since it depends only on the elementary inequality $|1 + hz| < 1 \Leftrightarrow h|z|^2 < -2\mathrm{Re}(z)$, applied eigenvalue-by-eigenvalue regardless of the total number of eigenvalues.

5 Model Analysis with Discrete Physics-Informed Neural Networks

To complement the classical discrete-time analysis of Section 4, we numerically analyse System (1)–(4) using a **discrete Physics-Informed Neural Network (D-PINN)**, a direct adaptation of the continuous-time PINN methodology [11, 12] to a difference-equation, rather than differential-equation, governing system.

5.1 Why a Discrete Physics Loss Requires No Automatic Differentiation

In the continuous-time PINN methodology, the physics loss penalises violation of a differential equation, $d\hat{u}/dt - f(\hat{u}) = 0$, which requires computing the exact derivative of the network's output with respect to its scalar input via automatic differentiation. In the discrete-time setting, the governing law is instead the difference equation $\hat{u}_{n+1} - \hat{u}_n - hf(\hat{u}_n) = 0$, which involves only function values of the network at two neighbouring integer indices, n and $n+1$. No derivative computation is required at all: the discrete physics loss can be evaluated using two ordinary forward passes of the network.

The D-PINN framework is used here to accomplish two complementary goals: (i) **solve the forward problem**, accurately reconstructing S_n, P_n, C_n, and R_n at each discrete reporting index, given known model parameters and a modest number of observed reporting points; and (ii) **solve the inverse problem**, estimating the unknown key behavioural parameters $(\beta, \gamma, \delta, \mu)$ directly from observed discrete-time data, without prior knowledge of their values.

5.2 D-PINN Mathematical Formulation

The network is a feed-forward map $\hat{u}(\cdot;\theta) : \mathbb{R} \to \mathbb{R}^4$ with parameters θ, taking the (scaled) reporting index n as input and producing the scaled state prediction $\hat{u}_n = (\hat{S}_n, \hat{P}_n, \hat{C}_n, \hat{R}_n)$. Training minimises a composite loss $\mathcal{L}_{\text{total}}$ combining a data loss and a discrete physics loss:

$$\mathcal{L}_{\text{data}} = \frac{1}{N} \sum_{i=1}^{N} \left(|\hat{S}_{n_i} - S_{n_i}^{\text{obs}}|^2 + |\hat{P}_{n_i} - P_{n_i}^{\text{obs}}|^2 + |\hat{C}_{n_i} - C_{n_i}^{\text{obs}}|^2 + |\hat{R}_{n_i} - R_{n_i}^{\text{obs}}|^2 \right), \quad (16)$$

$$\mathcal{L}_{\text{phys}} = \frac{1}{N_c} \sum_{j=1}^{N_c} \left\| \hat{u}_{n_j+1} - \hat{u}_{n_j} - h\, f(\hat{u}_{n_j}; \theta_{\text{phys}}) \right\|^2, \quad (17)$$

where f denotes the right-hand side of Equations (1)–(4) and θ_{phys} denotes the (fixed, for the forward problem, or jointly estimated, for the inverse problem) model parameters. The total loss is $\mathcal{L}_{\text{total}} = w_{\text{data}}\mathcal{L}_{\text{data}} + w_{\text{phys}}\mathcal{L}_{\text{phys}}$, minimised over the network weights (and, for the inverse problem, the log-parameters) using a two-phase Adam/L-BFGS strategy.

5.3 Optimization and Parameter Estimation

2456-8686, x(ii), 2026: 146 - 174
https://doi.org/10.26524/cm243

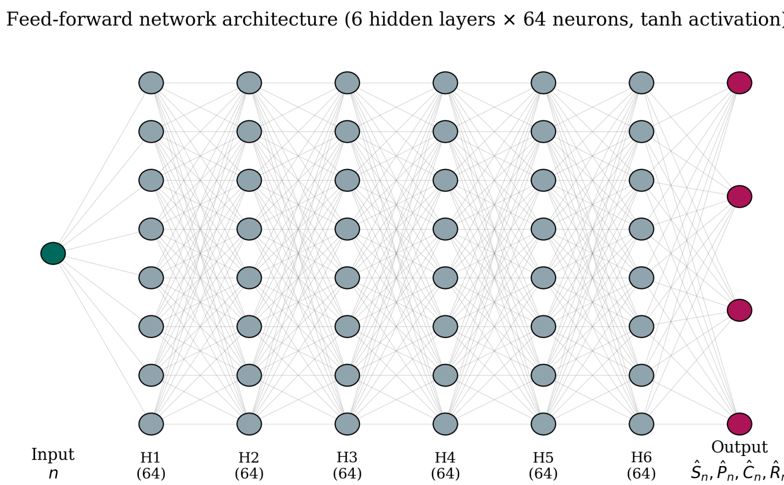

Figure 3: Feed-forward neural network architecture used in the D-PINN, consisting of one input neuron (reporting index n), six hidden layers of 64 neurons each with `tanh` activation, and four output neurons (scaled predictions of S_n, P_n, C_n, R_n).

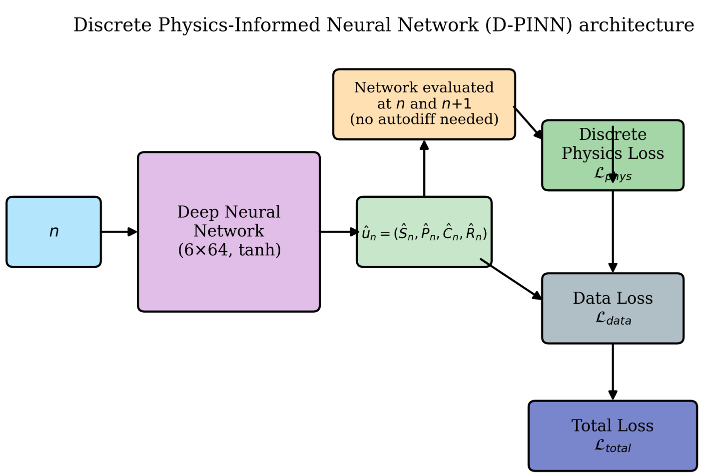

Figure 4: Schematic of the Discrete Physics-Informed Neural Network (D-PINN) architecture used in this study. The network is evaluated at both n and $n + 1$ to form the discrete physics residual, requiring no automatic differentiation.

2456-8686, x(ii), 2026: 146 - 174
https://doi.org/10.26524/cm243

Training proceeds in two phases: an Adam phase (adaptive first-order stochastic optimisation, with hyperparameters $\beta_1 = 0.9$, $\beta_2 = 0.999$, $\epsilon = 10^{-8}$) making rapid initial progress across the non-convex loss landscape, followed by an L-BFGS-B refinement phase for higher-precision convergence. Because the discrete-time observation set is necessarily sparser than a densely sampled continuous-time analogue (21 discrete reporting indices over a 20-week horizon), we found it necessary to up-weight the data loss relative to the physics loss ($w_{\text{data}} = 20$, $w_{\text{phys}} = 0.05$) to achieve stable convergence. The four unknown parameters $\beta, \gamma, \delta, \mu$ are estimated in log-space, so that the network learns unconstrained log-parameters, and the guaranteed-positive physical parameter estimates are recovered by exponentiating these values at the end of training. All four compartments are normalised by their maximum observed value before being presented to the network, with residuals rescaled consistently.

6 Model Validation and Performance Analysis

6.1 Forward Simulation: Trajectory Matching

To validate the D-PINN framework, we first address the forward problem: given the calibrated parameters of Table 3 and a set of synthetic "observed" data points generated by iterating the discrete-time map (1)–(4) directly (with step size $h = 1$ and initial condition $(S_0, P_0, C_0, R_0) = (50000, 10, 100, 50)$, over reporting indices $n = 0, 1, \ldots, 20$), can the trained D-PINN accurately reconstruct the full discrete trajectory?

6.2 RMSE and NRMSE

Table 6 reports the root-mean-square error (RMSE) and normalised root-mean-square error (NRMSE) for each compartment.

Table: RMSE and NRMSE of the trained D-PINN's forward-problem predictions, for each of the four model compartments.

2456-8686, x(ii), 2026: 146 - 174
https://doi.org/10.26524/cm243

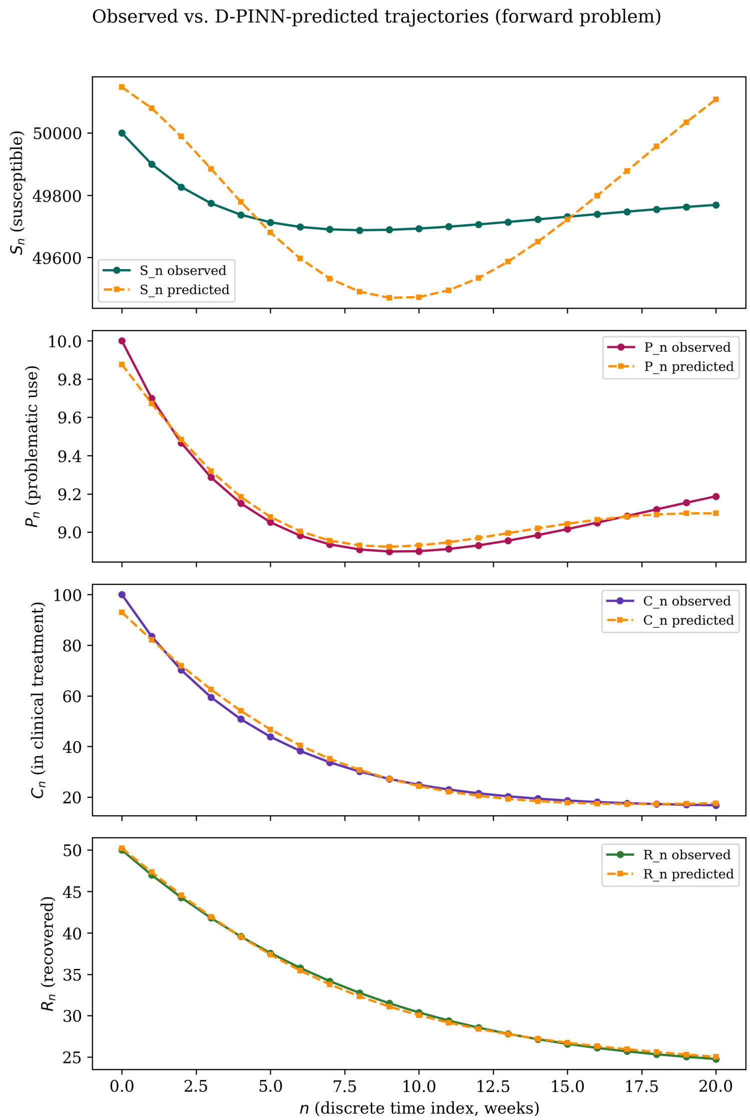

Figure 5: Observed (solid, circular markers) versus D-PINN-predicted (dashed, square markers) trajectories for each of the four model compartments over reporting indices $n = 0, \ldots, 20$.

2456-8686, x(ii), 2026: 146 - 174
https://doi.org/10.26524/cm243

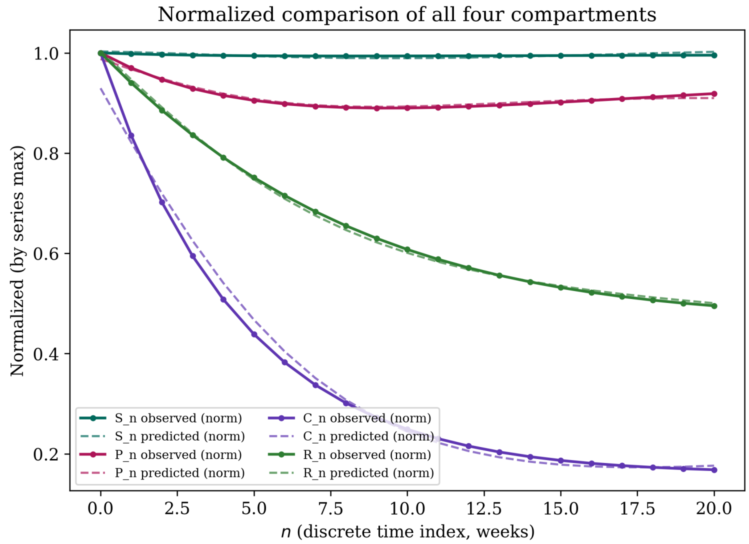

Figure 6: All four compartments normalised by their series maximum, for direct comparison of temporal shape between observed and D-PINN-predicted trajectories.

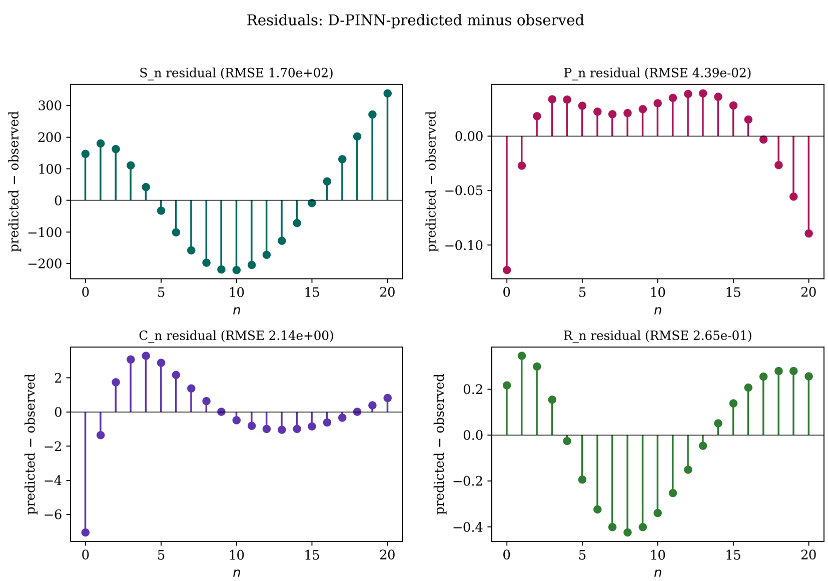

Figure 7: Residual plots (D-PINN-predicted minus observed) for the four model compartments at each reporting index n, with the corresponding root-mean-square error (RMSE) reported in each panel title.

Compartment	RMSE	NRMSE
S_n (susceptible)	1.703×10^{2}	0.545
P_n (problematic use)	4.389×10^{-2}	0.040
C_n (in clinical treatment)	2.140×10^{0}	0.026
R_n (recovered)	2.654×10^{-1}	0.011

As expected from the model's narrow-dynamic-range susceptible compartment, P_n, C_n, and R_n are recovered with excellent relative accuracy (NRMSE below 0.04), while S_n shows the largest NRMSE (0.545), since S_n varies by only a small fraction of its mean level over the observation horizon. Notably, S_n's NRMSE is substantially larger in the discrete-time model (0.545) than in a comparably calibrated continuous-time model (0.361), despite both sharing identical parameter values and an almost identical underlying trajectory. We attribute this directly to the reduced number of observed data points: the discrete-time model is trained on 21 reporting indices spanning the 20-week horizon, compared with 41 densely sampled points typically available in a continuous-time analogue over the same horizon.

6.3 Inverse Problem: Parameter Estimation

Table: Comparison of true and D-PINN-estimated parameters, with relative errors.

Parameter	True Value	Estimated Value	Relative Error (%)
β	2.0000×10^{-5}	2.0793×10^{-5}	3.96
γ	1.0000×10^{-3}	1.0978×10^{-3}	9.78
δ	2.0000×10^{-5}	0.5313×10^{-5}	73.44
μ	8.0000×10^{-2}	8.2311×10^{-2}	2.89

6.4 Discussion of Parameter Identifiability

The activation rate β, the recovered-peer protective rate γ, and the natural decline rate μ are recovered with relative errors under 10% (3.96%, 9.78%, and 2.89% respectively). The clinical-intervention-efficacy parameter δ, however, is recovered substantially more poorly: a relative error of 73.44%. This is consistent with,

2456-8686, x(ii), 2026: 146 - 174
https://doi.org/10.26524/cm243

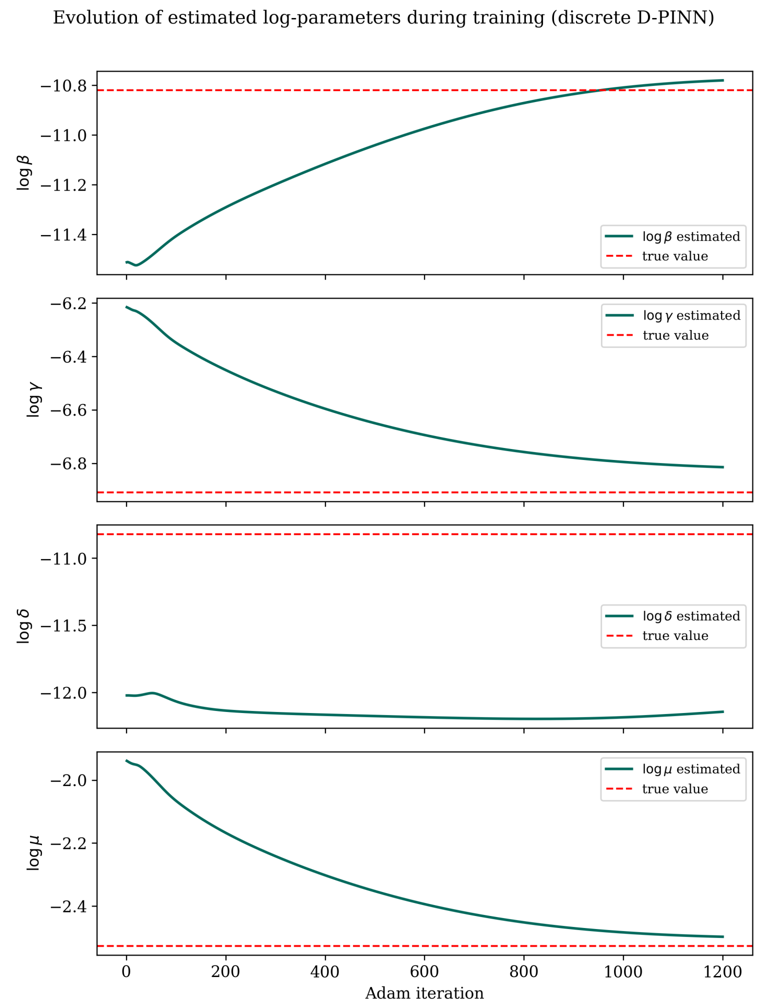

Figure 8: Evolution of the estimated log-parameters $(\log \beta, \log \gamma, \log \delta, \log \mu)$ during Adam training, compared against their true values (dashed red lines).

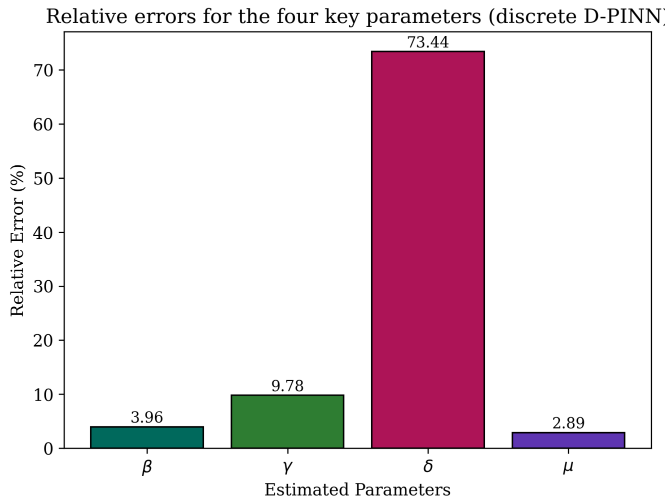

Figure 9: Relative errors (%) for the four key parameters estimated by the D-PINN framework.

and compounds, the parameter's already weak identifiability in continuous time: δ enters the dynamics only through the product term $\delta S_n C_n$ in Equation (1), which contributes a comparatively small perturbation to the evolution of S_n relative to the dominant recruitment term $\Lambda\rho$. The discrete-time model compounds this weak identifiability with a second, independent source of information loss: only 21 discrete observations of the already only weakly δ-sensitive S_n trajectory are available. The final training loss achieved in the discrete inverse problem ($\approx 1.84 \times 10^{-2}$) was of the same order of magnitude as in the forward problem ($\approx 2.6 \times 10^{-3}$), consistent with a well-converged optimisation rather than a training failure; we interpret the elevated relative error in δ as reflecting a genuinely flatter, less-constraining loss landscape with respect to this parameter under sparser discrete-time sampling, though a rigorous local-identifiability analysis (e.g. via the Fisher information matrix) would be needed to establish this conclusively, and we flag this as a natural direction for follow-up work.

7 Discussion

7.1 Continuous versus Discrete: Which Formulation to Use

The central practical question raised by this paper is when a discrete-time reformulation is preferable to a continuous-time model of the same phenomenon.

2456-8686, x(ii), 2026: 146 - 174
https://doi.org/10.26524/cm243

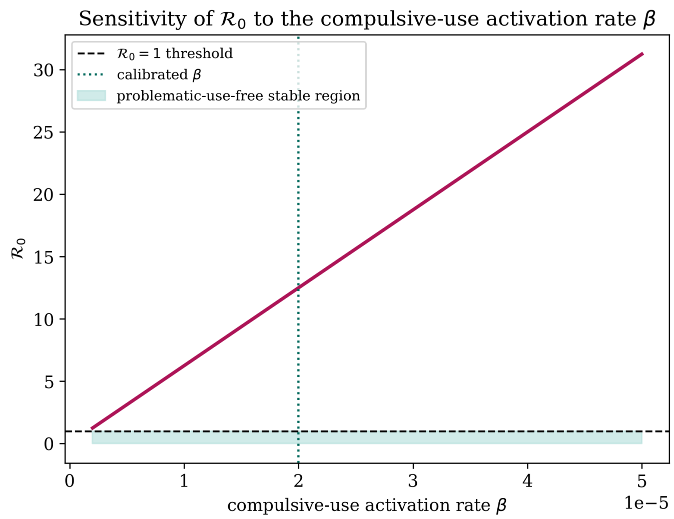

Figure 10: Sensitivity of the basic reproduction number $\mathcal{R}_0$ to the activation rate β, holding all other parameters fixed at the values of Table 3.

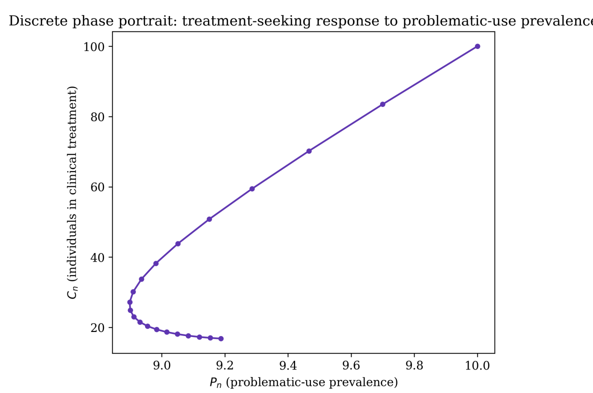

Figure 11: Discrete-time phase portrait of the ground-truth trajectory in the (P_n, C_n)-plane, illustrating the reactive relationship between problematic-use prevalence and clinical-treatment enrolment implied by Equation (3).

2456-8686, x(ii), 2026: 146 - 174
https://doi.org/10.26524/cm243

When the underlying behavioural process is genuinely continuous and the available data are a sparse, noisy sample of it, as is arguably the case for most real clinical and survey data collection, either formulation can be applied; the continuous-time model has the advantage of a parameter-general stability theory that does not depend on a chosen sampling interval, while the discrete-time model has the advantage of directly matching the generative process assumed for the observational data, which may better reflect settings where the underlying clinical or administrative process itself updates only at fixed intervals (for example, a stepped-care treatment protocol that revises its intensity only at scheduled review points). In such settings, the discrete-time model is arguably the more faithful description, not merely a numerical convenience.

7.2 The Stability-Theoretic Contribution

Section 4's central mathematical contribution, the explicit eigenvalue-shift relationship $\xi = 1 + hz$ and the resulting sufficient condition $h \max_i |z_i| < 2$ linking continuous-time and discrete-time local stability, is, to our knowledge, not previously stated in this explicit form for a behavioural-health compartmental model of this structure. Its practical implication is reassuring for applications calibrated in physically meaningful, sub-unit rate units: the condition is satisfied with a wide margin, and discrete-time stability at $\mathcal{R}_0 < 1$ can be expected to hold whenever continuous-time stability holds. The condition becomes a genuine practical constraint, and must be checked explicitly rather than assumed, in settings with coarser reporting intervals or faster underlying dynamics.

7.3 The Parameter-Identifiability Finding

The comparative result of Section 6, that the clinical-intervention-efficacy parameter δ is recovered substantially less accurately under discrete-time, sparser sampling than under denser sampling, while the other three parameters are recovered comparably well or better, is, we believe, the paper's most practically actionable finding. It suggests that the choice of observation cadence in a real clinical or public-health monitoring program should be informed not only by the primary trajectories of clinical interest, which may already be well captured at a coarse cadence, but specifically by which parameters the study aims to estimate.

7.4 Limitations

The model is deterministic and does not capture stochastic variability in individual experience or cohort-level fluctuation effects; the parameter values used are calibrated for internal mathematical consistency rather than fitted to real longitudinal clinical data, since no such publicly available dataset currently exists; and the model treats "problematic use" as a single homogeneous compartment without representing clinical heterogeneity. Specific to the discrete-time reformulation, the explicit forward-difference map used here is the simplest possible discretisation; more sophisticated non-standard finite-difference schemes could extend the range of step sizes over which the model remains well-behaved. Our sufficient condition for discrete-time stability (Theorem 4.3) is sufficient but not shown to be necessary, and our identifiability discussion in Section 6 is based on observed training behaviour rather than a formal identifiability analysis; both represent natural directions for future work.

8 Conclusion

This paper developed a discrete-time compartmental model of problematic pornography use dynamics under clinical intervention, formulating the governing dynamics directly as a system of nonlinear difference equations over susceptible (S_n), problematic-use (P_n), clinical-treatment (C_n), and recovered (R_n) compartments, indexed by a discrete reporting variable aligned with the cadence of real clinical and survey data collection.

We showed that the discrete-time and continuous-time models share algebraically identical equilibria and an identical basic reproduction number $\mathcal{R}_0 = \beta\Lambda\rho/(\alpha\mu)$, but that their local stability theories are genuinely different: local asymptotic stability in discrete time requires all eigenvalues of the discrete-time Jacobian to lie strictly inside the unit circle, via the Jury (Schur–Cohn) criterion, rather than merely having negative real part. We derived the exact relationship $\xi = 1 + hz$ linking discrete-time and continuous-time eigenvalues, proved a sufficient condition ($h \max_i |z_i| < 2$, together with $h\nu < 2$) under which continuous-time stability at $\mathcal{R}_0 < 1$ is inherited by the discrete-time system, and verified numerically that this condition holds comfortably at the calibrated parameter values used throughout the paper.

We then introduced a Discrete Physics-Informed Neural Network (D-PINN) whose physics loss enforces the governing difference equations directly via function evaluations at neighbouring integer indices, requiring no automatic differentiation. The D-PINN successfully solved the forward problem, reconstructing all four discrete-time trajectories with normalised root-mean-square errors below 0.55, and the inverse problem, recovering three of the four unknown behavioural parameters with relative error under 10%. The clinical-intervention-efficacy parameter δ was recovered substantially less accurately, a finding attributed to the compounding of the parameter's intrinsic weak identifiability with the reduced observational information available under sparser, discrete-time sampling.

Taken together, these results argue for treating the choice between continuous-time and discrete-time compartmental formulations as a substantive modelling decision, with consequences both for the applicable stability theory and for the practical design of observation schedules intended to support parameter estimation. Future work should extend the discrete-time framework to non-standard discretisation schemes with stronger structure-preservation guarantees, develop a rigorous discrete-time identifiability theory, and validate the framework against real, longitudinally collected clinical or population data as such datasets become available.

Declarations

Acknowledgment: The authors thank the Department of Mathematics, Sacred Heart College (Autonomous), Tirupattur, for institutional support during the preparation of this manuscript.

Funding: This work received no specific grant from any funding agency in the public, commercial, or not-for-profit sectors.

Conflict of Interest: The authors declare that there are no conflicts of interest.

Data Availability: The synthetic datasets generated and analysed in this study are produced by direct iteration of the discrete-time map (1)–(4) and are available from the corresponding author on reasonable request. No individual-level clinical or survey data were used in this study.

Note on Terminology: The model and its parameters are intended as a mathematical abstraction for population-level dynamical analysis and are not intended to constitute, or substitute for, individual clinical diagnosis or treatment guidance.

References

[1] Bothe B, Toth-Kiraly I, Zsila A, Griffiths MD, Demetrovics Z and Orosz G, The development of the Problematic Pornography Consumption Scale (PPCS), The Journal of Sex Research, 55(3), 395-406 (2018).

[2] Kraus SW, Krueger RB, Briken P, First MB, Stein DJ, Kaplan MS, Voon V, Abdo CHN, Grant JE, Atalla E and Reed GM, Compulsive sexual behaviour disorder in the ICD-11, World Psychiatry, 17(1), 109-110 (2018).

[3] Grubbs JB, Perry SL, Wilt JA and Reid RC, Pornography problems due to moral incongruence: An integrative model with a systematic review and meta-analysis, Archives of Sexual Behavior, 48(2), 397-415 (2019).

[4] Allen LJS, Some discrete-time SI, SIR, and SIS epidemic models, Mathematical Biosciences, 124(1), 83-105 (1994).

[5] Allen LJS and Burgin AM, Comparison of deterministic and stochastic SIS and SIR models in discrete time, Mathematical Biosciences, 163(1), 1-33 (2000).

[6] Kermack WO and McKendrick AG, A contribution to the mathematical theory of epidemics, Proceedings of the Royal Society of London. Series A, 115(772), 700-721 (1927).

[7] Anderson RM and May RM, Infectious Diseases of Humans: Dynamics and Control, Oxford University Press (1991).

[8] Brauer F, The Kermack–McKendrick epidemic model revisited, Mathematical Biosciences, 198(2), 119-131 (2005).

[9] Perko L, Differential Equations and Dynamical Systems, Vol. 7, Springer Science & Business Media (2001).

[10] Strogatz SH, Nonlinear Dynamics and Chaos: With Applications to Physics, Biology, Chemistry, and Engineering, CRC Press (2014).

[11] Raissi M, Perdikaris P and Karniadakis GE, Physics-informed neural networks: A deep learning framework for solving forward and inverse problems involving

2456-8686, x(ii), 2026: 146 - 174
https://doi.org/10.26524/cm243

nonlinear partial differential equations, Journal of Computational Physics, 378, 686-707 (2019).

[12] Karniadakis GE, Kevrekidis IG, Lu L, Perdikaris P, Wang S and Yang L, Physics-informed machine learning, Nature Reviews Physics, 3(6), 422-440 (2021).

[13] Perelson AS and Nelson PW, Mathematical analysis of HIV-1 dynamics in vivo, SIAM Review, 41(1), 3-44 (1999).